VPI-E-71-9
June 1971

Two Stochastic Models for Simulation of Correlated Random Processes

M. Hoshiya and H. W. Tieleman
Department of Engineering Mechanics

This research was supported by the National Aeronautics and Space Administration, Washington, D. C. under Grant No. NGL 47-004-067.

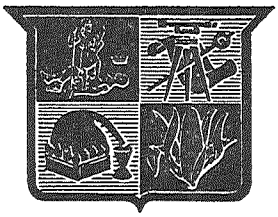

College of Engineering,
Virginia Polytechnic Institute
and State University

TWO STOCHASTIC MODELS FOR SIMULATION OF CORRELATED RANDOM PROCESSES

M. Hoshiya*

and

H. W. Tieleman**

Department of Engineering Mechanics
College of Engineering
Virginia Polytechnic Institute and State University
Blacksburg, Virginia 24061

---

*Assistant Professor

**Assistant Professor

ABSTRACT

In this technical report two methods are described to simulate a set of two correlated stationary and Gaussian processes with zero mean. The first method utilizes an exponential model with a uniformly distributed phase angle. The second method utilizes a trigonometric model with randomly varying amplitudes with Gaussian probability density functions. In both cases the simulation can be achieved on the basis of known power spectral density functions of each of the random processes and their cross-spectral density functions. The random variables in the expressions describing the random process are generated with the use of established Monte Carlo techniques.

The two methods are used for the simulation of two correlated stream wise turbulence components in the surface layer of the atmospheric boundary layer. These two turbulence components are taken at two different points A and B such that the separation distance A B lies in the horizontal plane normal to the direction of the mean wind.

Autocorrelation functions, spectra, cross-correlation functions, cross-spectral density functions and coherence functions are calculated numerically for each of the two sets of generated time histories and compared with the original spectrum functions and coherence function from which these time histories were generated.

CONTENTS

FIGURES

NOMENCLATURE

A_j, θ_j	Polar form of complex variable a_j
a_j, b_j, c_j, d_j	Amplitude
a_{xyj}	Real variable related to the coherence function
$C_{xy}(\omega)$	Co-spectral density function
C_{xyj}	Covariance
E [ ]	Expectation
f	Frequency
i	$\sqrt{-1}$
j, k	Positive Integer
k'	Dimensionless coefficient
n	Number of terms in series representation of the random processes
P (/)	Conditional probability distribution function
p (/)	Conditional probability density function
p ( )	Probability density function
p (,)	Joint probability density function
$Q_{xy}(\omega)$	Quadrature spectral density function
$R_x(\tau)$, $R_y(\tau)$	Autocorrelation function
$R'(\tau)$	Autocorrelation coefficient
$R_{xy}(\tau)$, $R_{yx}(\tau)$	Cross correlation function
$S_y(\omega)$, $S_x(\omega)$	Power spectral density function
$S'_u(f)$	One-sided strong-wind spectrum
$S_{xy}(\omega)$	Cross-spectral density function
t	Time
Δt	Time interval
U,V,W	Velocity components
$\overline{U}$,$\overline{W}$	Mean velocity components

u,v,w	Fluctuating velocity components
$\bar{U}_1$	Reference velocity
u^1	Upper bound
$x(t)$, $y(t)$	Random process
x	$\frac{1200f}{\bar{U}_1}$
x'	$\frac{600\omega}{\pi\bar{U}_1}$
Δy	Lateral separation distance
α_j, ϕ_j, η_j	Phase angles
$\gamma_{xy}(\omega)$	Coherence function
$\delta(\ )$	Dirac delta function
K	Drag coefficients
ρ	Density of air
ρ_{xyj}	Correlation coefficient
σ_{xj}, σ_{yj}	Standard deviation
τ	Time lag
τ'	Shear stress
ω_j	Wave number
$\Delta\omega$	Wave number interval

Subscripts

ℓ	Lower limit
u	Upper limit

Superscripts

C	Continuous
D	Discrete
*	Complex conjugate

I. INTRODUCTION

Trigonometric series (Ref. 1), filtered white noise (Ref. 2), filtered shot noise (Ref. 3) and correlated random pulse trains (Ref. 4) can be used as models for simulation of a single stochastic process such as earthquake waves. In order to simulate two correlated stochastic processes with arbitrary spectra, only the first method can be used.

Under strong wind conditions the turbulence components in the atmospheric surface layer are mainly due to frictional effects. The streamwise component of the turbulence may under certain conditions be approximated by a stationary Gaussian process with zero mean over a time interval of 1/2 hour to 1 hour (Ref. 5). This technical report employs stochastic models for the purpose of simulating a set of spatially correlated turbulence time histories. Statistical quantities of atmospheric turbulence have been studied for various atmospheric conditions and general empirical expressions for these quantities are becoming available. Based on this information two methods will be described in this report which will enable us to simulate the actual time histories. These simulation methods may be extremely powerful tools in the fields of weather forecasting and industrial aerodynamics for example. Since, two correlated stochastic processes with arbitrary spectra and coherence function can be simulated, the described methods may be applied to any physical phenomenon as long as the process can be assumed to be stationary and Gaussian.

II. EXPONENTIAL MODEL WITH UNIFORMLY DISTRIBUTED PHASE ANGLE.

Assume that the random process $x(t)$ can be expressed in the following mathematical form,

$$x(t) = \sum_{j=-n}^{n} a_j \, e^{i(\omega_j t + \phi_j)} \tag{1}$$

The amplitude a_j is in general complex and symmetrical with respect to j so that

$$a_{-j} = a_j^* \quad \text{and} \quad a_o = o$$

where a_j^* is the complex conjugate of a_j and n is some large positive integer.

Furthermore, ω_j is a set of real variables representing the wave number with

$$\omega_{-j} = - \omega_j$$

and ϕ_j represents the phase angles, each of which is assumed to be a random variable with a uniform probability density function over the range from zero to 2π. Also ϕ_j is odd with respect to the index j and consequently

$$\phi_{-j} = - \phi_j .$$

Let $a_j = A_j \, e^{i\theta_j}$, where A_j and θ_j both are real, then

$$A_{-j} = A_j, \; \theta_{-j} = - \theta_j \text{ and } A_o = o.$$

It is also assumed that the phase angles are statistically independent. With the above assumptions expression (1) can now be written as

$$x(t) = 2 \sum_{j=1}^{n} A_j \cos (\omega_j t + \theta_j + \phi_j), \tag{2}$$

where A_j, ω_j and θ_j are real and deterministic variables and ϕ_j is a real and random variable. Consequently, $x(t)$ represents a random process. As a matter of fact, $x(t)$ represents a stationary Gaussian process with zero mean as will be shown next. Consider the random process as an

infinite ensemble of sample functions; then the ensemble average or the expectation of x(t) is defined as

$$E\,[x(t)] = \int_{-\infty}^{+\infty} x\, p(x)\, dx$$

where p(x) is the probability density function which is always a real-valued, non-negative function. The expected value of x(t) in equation (1) is

$$E\,[x(t)] = \sum_{j=-n}^{n} a_j\, e^{i\omega_j t}\; E\left[e^{i\phi_j}\right]$$

since it was assumed that ϕ_j had a uniform probability density function over the range from o to 2π.

$$E\,[e^{i\phi_j}] = E\,[\cos\phi_j] + i\,E\,[\sin\phi_j]$$
$$= \frac{1}{2\pi}\int_{o}^{2\pi} \cos\phi_j\, d\phi_j + i\,\frac{1}{2\pi}\int_{o}^{2\pi} \sin\phi_j\, d\phi_j = 0.$$

Consequently, E [x(t)] = 0, and x(t) has a zero mean value.

Next we will show that the autocorrelation function is a function of time-lag only and therefore x(t) is a stationary process. The autocorrelation function of x(t) is defined by the expectation of the product of $x(t+\tau)$ and $x^*(t)$. Using expression (1)

$$E\,[x(t+\tau)\; x^*(t)] = E\left[\sum_{j=-n}^{n} a_j\, e^{i(\omega_j t + \omega_j \tau + \phi_j)} \sum_{k=-n}^{n} a_k^*\, e^{-i(\omega_k t + \phi_k)}\right]$$

and

$$E\,[x(t+\tau)\; x^*(t)] = \sum_{\substack{j=-n \\ (j=k)}}^{n} a_j\, a_j^*\, e^{i\omega_j \tau} + \sum_{j=-n}^{n}\sum_{\substack{k=-n \\ (j\neq k)}}^{n} a_j\, a_k^*\, e^{i(\omega_j t - \omega_k t + \omega_j \tau)}\; E\left[e^{i(\phi_j - \phi_k)}\right]$$

Due to the fact that ϕ_j and ϕ_k are independent for $j \neq k$

$$E\left[e^{i(\phi_j - \phi_k)}\right] = 0$$

Consequently,

$$R_x(\tau) = E\,[x(t+\tau)\; x^*(t)] = \sum_{j=-n}^{n} a_j\, a_j^*\; e^{i\omega_j \tau} \tag{3}$$

It can be easily verified that $R_x(\tau)$ is an even and real function of τ since

$$R_x(\tau) = R_x(-\tau) \quad \text{and} \quad R_x(\tau) = R_x^*(\tau)$$

Since the random variable x(t) at a specified time is defined as the sum of n independent identically-distributed random-variables, the central limit theorem states that if n approaches infinity, the probability density function of x approaches the probability density function of a Gaussian random variable. Consequently the random process x(t) as defined by equation (1) represents a stationary Gaussian process with a zero mean if n approaches infinity.

The spectral density function of x(t) can now be obtained by taking the Fourier transform of $R_x(\tau)$ using expression (3)

$$S_x(\omega) = \frac{1}{2\pi} \int_{-\infty}^{+\infty} R_x(\tau)\; e^{-i\omega\tau}\; d\tau = \frac{1}{2\pi} \sum_{j=-n}^{n} a_j\, a_j^* \int_{\infty}^{+\infty} e^{-i(\omega-\omega_j)\tau}\; d\tau$$

or

$$S_x(\omega) = \sum_{j=-n}^{n} a_j\, a_j^*\; \delta(\omega-\omega_j). \tag{4}$$

Where $\delta(\omega-\omega_j)$ is the Dirac delta function or unit impulse which has unit area concentrated above $\omega=\omega_j$ so that $\int_{-\infty}^{+\infty} \delta(\omega-\omega_j)\, d\omega = 1.0$ and $\delta(\omega-\omega_j) = \infty$ for $\omega = \omega_j$ and zero for $\omega \neq \omega_j$. This form of the power spectrum is a sequence of impulses, which one would expect to obtain because the original equation for x(t) takes only discrete values for ω. The area under each

impulse equals the area under $S_x^C(\omega)$ in an interval of length $\Delta\omega$ (Figure 1). Consequently the Fourier transform can not be continuous. However the power spectrum density functions of a physical random process x(t) should be continuous and given by $S_x^C(\omega)$. The discrete form of the spectrum is given by

$$S_x^D(\omega) = \sum_{j=-n}^{n} S_x^C(\omega_j)\ \delta(\omega-\omega_j)\Delta\omega \tag{5}$$

where $\Delta\omega = \frac{\omega_u - \omega_\ell}{n-1}$ and $\omega_j = \omega_\ell + (j-1)\Delta\omega$.

A significant contribution to the variance of x(t) is obtained between the wave numbers ω_ℓ (lower limit) and ω_u (upper limit). Note that $S_x^D(\omega)$ represents the spectral intensity $S_x^C(\omega_j)\Delta\omega$ at $\omega = \omega_j$. By comparison of equations (4) and (5) one concludes that

$$a_j a_j^* = S_x^C(\omega_j)\Delta\omega \tag{6}$$

Consider now another stationary Gaussian process with zero mean:

$$y(t) = \sum_{j=-n}^{n} b_j\, e^{i(\omega_j t + \eta_j)} \tag{7}$$

which is defined in the same way as x(t) except that b_j is now real. As before, η_j is the random variable with a uniform probability density function over the range from zero to 2π. It is assumed that ϕ_j in Eq. (1) and η_j in Eq. (7) are statistically correlated. According to Parzen, (Ref. 6) the joint probability density function of ϕ_j and η_j can be written as

$$P(\phi_j, \eta_j) = \frac{1}{4\pi^2}\left\{1 + \frac{a_{xyj}}{\pi^2}\,[\phi_j - \pi]\,[\eta_j - \pi]\right\} \tag{8}$$

This expression is a possible form of the joint probability density function function of ϕ_j and η_j since it satisfies the properties of the definition of the joint probability density function.

$$\int_0^{2\pi} \int_0^{2\pi} p\ (\phi_j, \eta_j)\ d\phi_j\ d\eta_j = 1.0$$

$$\int_0^{2\pi} p\ (\phi_j, \eta_j)\ d\phi_j = p\ (\eta_j)$$

and $$\int_0^{2\pi} p\ (\phi_j, \eta_j)\ d\eta_j = p\ (\phi_j).$$

Since all ϕ_j's are independent and all η_k's are independent, ϕ_j and η_j for $j \neq k$ are also independent. Only when $j = k$ are ϕ_j and η_k statistically correlated. Since $p\ (\phi_{-j}, \eta_{-j}) = p\ (-\phi_j, -\eta_j)$ we may conclude from equation (8) that

$$a_{xyj} = a_{-xyj}.$$

The cross correlation function of x(t) and y(t) describes the general dependence of the values of x(t) on the values of y(t) and is defined as

$$E\ [x(t+\tau)\ y^*(t)] = E\ [\sum_{j=-n}^{n} a_j\ e^{i(\omega t+\omega_j\ \tau+\phi_j)} \sum_{k=-n}^{n} b_k\ e^{-i(\omega_k t+\eta_k)}]$$

or

$$E\ [x(t+\tau)\ y^*(t)] = \sum_{\substack{j=-n \\ j=k}}^{n} a_j\ b_j\ e^{i\omega_j\tau}\ E\ [e^{i(\phi_j\ -\ \eta_j)}]$$

$$+ \sum_{j=-n}^{n} \sum_{\substack{k=-n \\ j\neq k}}^{n} a_j\ b_k\ e^{i(\omega_j t\ +\ \omega_j\tau\ -\ \omega_k t)}\ E\ [e^{i(\phi_j\ -\ \eta_k)}]$$

However,

$$E\ [e^{i(\phi_j\ -\ \eta_j)}] = \int_0^{2\pi} \int_0^{2\pi} e^{i(\phi_j\ -\ \eta_j)}\ p\ (\phi_j, \eta_j)\ d\phi_j\ d\eta_j$$

After substitution of the expression (8) for the joint probability density curve, one obtains

$$E\left[e^{i(\phi_j - \eta_j)}\right] = \frac{a_{xyj}}{\pi^2} \tag{9}$$

Since ϕ_j and η_k for $j \neq k$ are independent we have

$$E\left[e^{i(\phi_j - \eta_k)}\right] = E\left[e^{i\phi_j}\right] \; E\left[e^{-i\eta_k}\right] = 0 \quad \text{for } j \neq k \tag{10}$$

Consequently the cross-correlation function for x(t) and y(t) becomes

$$E\left[x(t+\tau)\, y^*(t)\right] = \sum_{j=-n}^{n} \frac{a_j b_j a_{xyj}}{\pi^2} \; e^{i\omega_j \tau} = R_{xy}(\tau). \tag{11}$$

$R_{xy}(\tau)$ does not necessarily have a maximum at $\tau = 0$ as was true for the autocorrelation function, nor is $R_{xy}(\tau)$ an even function. However, $R_{xy}(\tau)$ does display symmetry about the ordinate when x and y are interchanged; that means that $R_{xy}(\tau) = R_{yx}(-\tau)$. Hence, the cross-spectral density function of x(t) and y(t), which is the Fourier transform of the cross-correlation function, is in general a complex function and is given by:

$$S_{xy}(\omega) = \frac{1}{2\pi} \int_{-\infty}^{+\infty} R_{xy}(\tau) \; e^{-i\omega\tau} \; d\tau \tag{12}$$

Substitution of Eq. (11) in Eq. (12) leads to

$$S_{xy}(\omega) = \sum_{j=-n}^{n} \frac{a_j b_j a_{xyj}}{\pi^2} \; \delta(\omega - \omega_j) \tag{13}$$

which is a complex function and can be written

$$S_{xy}(\omega) = C_{xy}(\omega) - i\, Q_{xy}(\omega)$$

Using the transformation $a_j = A_j\, e^{i\theta_j}$

$$C_{xy}(\omega) = \sum_{j=-n}^{n} \frac{A_j b_j a_{xyj}}{\pi^2} \; \delta(\omega - \omega_j) \cos\theta_j \tag{14}$$

and $$Q_{xy}(\omega) = -\sum_{j=-n}^{n} \frac{A_j b_j a_{xyj}}{\pi^2} \; \delta(\omega - \omega_j) \sin\theta_j \tag{15}$$

The real part of the cross-correlation function is called the co-spectral density function and the imaginary part of the quadrature spectral density function. Similar to the derivation of expression (6) it can be shown that

$$C^{C}_{xy}\ (\omega_j)\ \Delta\omega = \frac{A_j b_j a_{xyj}}{\pi^2}\ \cos\theta_j \tag{16}$$

and $$Q^{C}_{xy}\ (\omega_j)\ \Delta\omega = -\frac{A_j b_j\ a_{xyj}}{\pi^2}\ \sin\theta_j \tag{17}$$

where the superscript C refers to the continuous spectrum functions. Solving for a_{xyj} and using (6) one gets:

$$a^2_{xyj} = \frac{\{[C^{C}_{xy}\ (\omega_j)]^2\ (\Delta\omega)^2 + [Q^{C}_{xy}\ (\omega_j)]^2\ (\Delta\omega)^2\}\ \pi^4}{A_j^2\ b_j^2} \qquad \text{or}$$

$$a^2_{xyj} = \frac{\pi^4 |S^{C}_{xy}(\omega_j)|^2}{S^{C}_{x}(\omega_j)\ \ S^{C}_{y}(\omega_j)}$$

Using the definition for the coherence function (Ref. 7)

$$\gamma^2_{xy}\ (\omega_j) \equiv \frac{|\ S^{C}_{xy}\ (\omega_j)\ |^2}{S^{C}_{x}\ (\omega_j)\ \ S^{C}_{y}\ (\omega_j)} \tag{18}$$

one obtains

$$a_{xyj} = \pi^2\ \ \gamma_{xy}\ (\omega_j) \tag{19}$$

Using expressions (16) and (17) one obtains

$$\theta_j = \tan^{-1}\ \{-\frac{Q^{C}_{xy}\ (\omega_j)}{C^{C}_{xy}\ (\omega_j)}\} \tag{20}$$

The procedure of simulation of a set of two correlated stationary Gaussian processes x(t) and y(t) will be described briefly using the so-called Monte Carlo method (see Refs. 8, 9 and 10). Since two

stochastic processes with arbitrary spectrum and coherence function can be produced, this method can be applied to any physical phenomena as long as the process can be assumed to be a stationary, Gaussian and has a zero mean. Using expressions (6), (19) and (20), A_j, b_j, a_{xyj} and θ_j can be obtained from the given spectrum functions

$$A_j = \sqrt{S_x^C(\omega_j)\Delta\omega}$$

$$b_j = \sqrt{S_y^C(\omega_j)\Delta\omega}$$

$$a_{xyj} = \pi^2 \frac{|S_{xy}^C(\omega_j)|}{\sqrt{S_x^C(\omega_j)}\sqrt{S_y^C(\omega_j)}} = \pi^2 \gamma_{xy}(\omega_j)$$

$$\text{and } \theta_j = \tan^{-1}\left\{-\frac{Q_{xy}^C(\omega_j)}{C_{xy}^C(\omega_j)}\right\}$$

where $j = 1, 2, 3 \_ \_ \_ \_ n$. The larger n, the more precise the random processes x(t) and y(t) can be simulated.

The next step is to generate a correlated pair of random variables ϕ_j and η_j for $j = 1, 2, \_ \_ \_ \_ n$ from the joint probability density function (8). This expression is the joint probability density function of two random variables ϕ_j and η_j each with a uniform probability density function over the interval from zero to 2π. This can be done as follows, (see Refs. 8 and 9):

Step 1.

A set of n independent random variables d_j is generated from a uniform probability density function over the interval from zero to one. Now a set of values of ϕ_j can be generated from $\phi_j = 2\pi d_j$ for $j = 1, 2, 3 \_ \_ \_ \_ n$.

Step 2.

From equation (8), the conditional probability distribution function of η_j is given by

$$P(\eta_j/\phi_j) = \int_o^{\eta_j} p(\eta_j/\phi_j)\, d\eta_j = \int_o^{\eta} \frac{p(\eta_j, \phi_j)}{p(\phi_j)}\, d\eta_j$$

or after substitution

$$P(\eta_j/\phi_j) = \frac{1}{2\pi}\eta_j + \frac{a_{xyj}}{2\pi^3}(\phi_j - \pi)\left(\frac{1}{2}\eta_j^2 - \pi\eta_j\right) \qquad (21)$$

Now another set of n independent random variables, e_j with a uniform probability density function over the interval from zero to one is generated. When the random variable e_j is equated to the conditional probability distribution function, one can solve for η_j when j = 1, 2, 3 _ _ _ _ n. Since this expression is quadratic in η_j, two solutions for η_j will be obtained. However, the value of η_j is chosen so that $o \leq \eta_j \leq u'$, where u' is the smaller positive value of 2π and $-\frac{2\pi}{a_{xyj}}$. If $a_{xyj} \geq o$ the upper bound is automatically 2π. The upper bounds are calculated from expression (21) for $\phi_j = 2\pi$ and $e_j = 1$.

The following procedure will be used to generate the time series x(t) and y(t). Given are the power spectral density functions of each of the two time series $S_x^C(\omega)$ and $S_y^C(\omega)$ and their cross-spectral density function $S_{xy}^C(\omega)$. The significant part of these spectra between a lower frequency ω_ℓ and an upper frequency ω_u, is subdivided in n-1 intervals of width $\Delta\omega$. The larger the value of n, the more accurately the time series will be simulated. The continuous spectrum functions are evaluated at the center of each interval such that $\omega_j = \omega_\ell + (j-1)\,\Delta\omega$. Using equations (6), (19) and (20), deterministic values for A_j, b_j, a_{xyj} and θ_j can be obtained for j = 1, 2 ____ n. The random variables ϕ_j and η_j are generated as

described in the above paragraph. We can now proceed to calculate a point of the random processes, say at time t_1, with

$$x(t_1) = 2 \sum_{j=1}^{n} A_j \cos (\omega_j + {}_1 + \theta_j + \phi_j)$$

$$y(t_1) = 2 \sum_{j=1}^{n} b_j \cos (\omega_j t_1 + \eta_j)$$

Next, the following point of the random processes can be calculated at time $t, + \Delta t$ and so on. The choice of the time interval depends on the value of the upper significant wave number and should be chosen such that

$$\Delta t \leq \frac{\pi}{\omega_u}.$$

III. TRIGONOMETRIC MODEL WITH NORMALLY DISTRIBUTED AMPLITUDE

Consider the following representation for the random process

$$x(t) = \sum_{j=1}^{n} (a_j \cos \omega_j t + b_j \sin \omega_j t) \tag{22}$$

where the coefficients a_j and b_j are independent random variables, each set with the same normal probability density function with standard deviation σ_x; and with zero mean. Furthermore, ω_j and t are deterministic representing the wave number and time respectively.

In the following section it will be shown that expression (22) represents a stationary Gaussian process with zero mean. The expected value of x(t) is

$$E[x(t)] = \sum_{j=1}^{n} \{E[a_j] \cos \omega_j t + E[b_j] \sin \omega_j t\}$$

since $E[a_j] = E[b_j] = 0$, $E[x(t)] = 0$.

The autocorrelation function for x(t) becomes:

$$E[x(t)\ x(t+\tau)] = \sum_{j=1}^{n} \sum_{k=1}^{n} E[a_j a_k] \cos \omega_j t \cos \omega_k (t+\tau) +$$

$$E[b_j a_k] \sin \omega_j t \cos \omega_k (t+\tau) +$$

$$E[a_j b_k] \cos \omega_j t \sin \omega_k (t+\tau) +$$

$$E[b_j b_k] \sin \omega_j t \sin \omega_k (t+\tau)$$

since b_j and a_k are independent for all values of j and k, one has

$$E[b_j a_k] = E[a_j b_k] = E[a_j]\ E[b_k] = 0.$$

Also

$$E[a_j a_k] = E[b_j b_k] = \sigma_{xj}^2 \text{ for } j = k \text{ and is zero for } j \neq k.$$

Consequently the autocorrelation becomes

$$E[x(t)\ x\ (t+\tau)] = \sum_{j=1}^{n} \sigma_{xj}^2 \cos (\omega_j \tau) = R_x (\tau). \tag{23}$$

The autocorrelation function $R_x(\tau)$ is independent of time t and depends on the time lag τ only. Also, the sum of a set of independent random variables with normal distribution gives rise to another random variable with a normal distribution. Consequently, x(t) represents a stationary Gaussian (normal) process with zero mean.

The power spectral density function can be obtained by taking the Fourier transform of $R_x(\tau)$

$$S_x(\omega) = \frac{1}{2\pi} \int_{-\infty}^{\infty} R_x (\tau)\ e^{-i\omega\tau}\ d\tau$$

Using (23) we have

$$S_x(\omega) = \frac{1}{2\pi} \int_{-\infty}^{\infty} \sum_{j=1}^{n} \sigma_{xj}^2 \cos (\omega_j \tau)\ e^{-i\omega\tau}\ d\tau$$

or

$$S_x(\omega) = \frac{1}{2\pi} \sum_{j=1}^{n} \sigma_{xj}^2 \int_{-\infty}^{\infty} \cos(\omega_j \tau) \cos \omega\tau \, d\tau.$$

Introducing the Dirac delta function

$$2\pi \, \delta(\omega-\omega_j) = \int_{-\infty}^{\infty} e^{-i(\omega-\omega_j)\tau} \, d\tau = \int_{-\infty}^{\infty} \cos \omega\tau \cos \omega_j \tau \, d\tau$$

$$+ \int_{\infty}^{\infty} \sin \omega\tau \sin \omega_j \tau \, d\tau$$

Similarly,

$$2\pi \, \delta(\omega+\omega_j) = \int_{-\infty}^{\infty} e^{i(\omega+\omega_j)\tau} \, d\tau = \int_{-\infty}^{\infty} \cos \omega\tau \cos \omega_j \tau d\tau$$

$$- \int_{-\infty}^{\infty} \sin \omega\tau \sin \omega_j \tau d\tau$$

Consequently,

$$\int_{-\infty}^{\infty} \cos \omega_j \tau \cos \omega\tau \, d\tau = \pi \{ \delta \omega-\omega_j) + \delta(\omega+\omega_j)\}$$

and the power spectral density function can be written as

$$S_x(\omega) = \frac{1}{2} \sum_{j=1}^{n} \sigma_{xj}^2 \{\delta (\omega-\omega_j) + \delta(\omega+\omega_j)\} \tag{24}$$

This expression gives the relation between the power spectral density function and the standard deviation σ_{xj} of the normal random variables with zero mean a_j and b_j.

Consider now another stationary Gaussian process with zero mean:

$$y(t) = \sum_{j=1}^{n} \{c_j \cos(\omega_j t + \alpha_j) + d_j \sin(\omega_j t + \alpha_j)\} \tag{25}$$

where the coefficients c_j and d_j are independent random variables, each set with the same normal probability density function with standard deviation σ_{yj}, and with zero mean. And α_j is deterministic, representing the phase angle. The two stationary normal processes are correlated if

there exists a non-zero correlation between a_j and c_j and/or b_j and d_j. The covariance C_{xyj} between two random variables a_j and c_j is defined as

$$C_{xyj} = E[a_j\, c_j]$$

Since a_j and b_j have the same standard deviation for the same j, and the same is true for the random variables c_j and d_j, the covariance between a_j and c_j must be equal to the covariance between b_j and d_j. The correlation coefficient is defined as

$$\rho_{xyj} = \frac{C_{xyj}}{\sigma_{xj}\sigma_{yj}} \tag{26}$$

and consequently

$$E[a_j c_j] = E[c_j d_j] = \rho_{xyj}\ \ \sigma_{xj}\ \ \sigma_{xj}$$

The cross-correlation function between the random process is

$$E[x(t)\ y(t+\tau] = \sum_{j=1}^{n}\ \sum_{k=1}^{n} \Big\{ E[a_j c_k]\ \cos(\omega_j t)\ \cos\ (\omega_k t + \omega_k \tau\ \ + \alpha_k) +$$

$$E[a_j d_k]\ \cos\ (\omega_j t)\ \sin\ (\omega_k t + \omega_k\ \tau\ \ + \alpha_k)\ \ +$$

$$E[b_j c_k]\ \sin\ (\omega_j t)\ \cos\ (\omega_k t + \omega_k \tau\ \ + \alpha_k) +$$

$$E[b_j d_k]\ \sin\ (\omega_j t)\ \sin\ (\omega_k t + \omega_k \tau\ \ +\ \ \alpha_k) \Big\}$$

Noting that $E[b_j c_k] = E[a_j d_k] = 0$ and

$$E[a_j c_k] = E[b_j d_k] = \sigma_{xj}\ \sigma_{yj}\ \ \rho_{xyj} \text{ for } j = k$$

and zero for $j \neq k$ the cross-correlation function becomes

$$E[x(t)\ y(t+\tau)] = \sum_{j=1}^{n} \sigma_{xj}\ \ \sigma_{yj}\ \ \rho_{xyj}\ \ \cos\ (\omega_j\ \tau + \alpha_j)$$

$$= R_{xy}\ (\tau) \tag{27}$$

In general, the cross-correlation function is not an even function of τ and its Fourier transform should be complex. The cross-spectral density function is defined as

$$S_{xy}(\omega) = \frac{1}{2\pi} \int_{-\infty}^{\infty} R_{xy}(\tau)\, e^{-i\omega\tau}\, d\tau$$

Substituting expression (27),

$$S_{xy}(\omega) = \frac{1}{2\pi} \sum_{j=1}^{n} \sigma_{xj}\, \sigma_{yj}\, \rho_{xyj} \int_{-\infty}^{\infty} \cos(\omega_j\tau + \alpha_j)\, e^{-i\omega\tau}\, d\tau \quad (28)$$

However,

$$\int_{-\infty}^{\infty} \cos(\omega_j\tau + \alpha_j)\, e^{-i\omega\tau}\, d\tau = \cos\alpha_j \int_{-\infty}^{\infty} \cos\omega_j\tau\, e^{-i\omega\tau}\, d\tau$$

$$- \sin\alpha_j \int_{-\infty}^{\infty} \sin\omega_j\tau\, e^{-i\omega\tau}\, d\tau$$

and

$$\int_{-\infty}^{\infty} \cos(\omega_j\tau + \alpha_j)\, e^{-i\omega\tau}\, d\tau = \cos\alpha_j \int_{-\infty}^{\infty} \cos\omega_j\tau \cos\omega\tau\, d\tau + i \sin$$

$$\alpha_j \int_{-\infty}^{\infty} \sin\omega_j\tau \sin\omega\tau\, d\tau$$

Introducing the Dirac delta function,

$$\int_{-\infty}^{\infty} \cos(\omega_j\tau + \alpha_j)\, e^{-i\omega\tau}\, d\tau = \pi \cos\alpha_j \{\delta(\omega-\omega_j) + \delta(\omega+\omega_j)\}$$

$$+ i\,\pi \sin\alpha_j \{\delta(\omega-\omega_j) - \delta(\omega+\omega_j)\}$$

The co-spectral density function becomes

$$C_{xy}(\omega) = \frac{1}{2} \sum_{j=1}^{n} \sigma_{xj}\, \sigma_{yj}\, \rho_{xyj} \cos\alpha_j \{\delta(\omega-\omega_j) + \delta(\omega+\omega_j)\}$$

and the quadration spectral density function becomes

$$Q_{xy}(\omega) = -\frac{1}{2} \sum_{j=1}^{n} \sigma_{xj}\, \sigma_{yj}\, \rho_{xyj} \sin\alpha_j \{\delta(\omega-\omega_j) - \delta(\omega+\omega_j)\}$$

The discrete form of the power spectrum is given by Eq. (5)

$$S_x^D(\omega) = \sum_{j=1}^{n} S_x^C(\omega_j)\ \delta(\omega-\omega_j)\ \Delta\omega \quad \text{for } \omega \geq 0$$

where $\Delta\omega = \frac{\omega_u - \omega_\ell}{n-1}$ and $\omega_j = \omega_\ell + (j-1)\ \Delta\omega$

comparing with equation (24) we have

$$\sigma_{xj} = \sqrt{2\ S_x^C(\omega_j)\ \Delta\omega} \tag{29}$$

Similarly:

$$\sigma_{yj} = \sqrt{2\ S_y^C(\omega_j)\ \Delta\omega} \tag{30}$$

From the expressions for the co-spectrum and quadrature spectrum

$$2\ C_{xy}^C(\omega_j)\ \Delta\omega = \sigma_{xj}\ \sigma_{yj}\ \rho_{xyj}\ \cos\alpha_j \tag{31}$$

and

$$2\ Q_{xy}^C(\omega_j)\ \Delta\omega = -\sigma_{xj}\ \sigma_{yj}\ \rho_{xyj}\ \sin\alpha_j \tag{32}$$

From Eq. (31) and Eq. (32)

$$\alpha_j = \tan^{-1}\left[-\frac{Q_{xy}^C(\omega_j)}{C_{xy}^C(\omega_j)}\right] \tag{33}$$

and from Eqs. (31), (32), (29) and (30)

$$\rho_{xyj}^2 = \frac{\{C_{xy}^C(\omega_j)\}^2 + \{Q_{xy}^C(\omega_j)\}^2}{S_x^C(\omega_j)\ S_y^C(\omega_j)} = \gamma_{xy}^2(\omega_j) \tag{34}$$

The last expression shows that the correlation coefficient ρ_{xyj} between the random variables is identical to the coherence function $\gamma_{xy}(\omega_j)$ of

the two random processes x(t) and y(t).

The next step is to generate independently, the random variables a_j and b_j from a normal distribution with zero mean and a standard deviation $\sigma_{xj} = \sqrt{2\, S_x^C(\omega_j)\, \Delta\omega}$ and $\sigma_{yj} = \sqrt{2\, S_y^C(\omega_j)\, \Delta\omega}$ respectively, for j = 1, 2, _ _ _ _, n. Again the larger n, the more precisely the random processes x(t) and y(t) will be simulated. The next step is to generate the random variables c_j and d_j from conditional normal distribution derived from the following considerations. Since a_j and c_j are both normally distributed, the joint probability density function of a_j and c_j is

$$P(a_j, c_j) = \frac{1}{2\pi\, \sigma_{xj}\, \sigma_{yj}\, \sqrt{1-\rho_{xyj}^2}} \exp\left\{ - \frac{1}{2(1-\rho_{xyj}^2)} \left[\frac{a_j^2}{\sigma_{xj}^2} - \frac{2\rho_{xyj}\, a_j\, c_j}{\sigma_{xj}\, \sigma_{yj}} + \frac{c_j^2}{\sigma_{yj}^2} \right] \right\} \tag{35}$$

and the probability density function of a_j is

$$P(a_j) = \frac{1}{\sqrt{2\pi}\, \sigma_{xj}} \exp\left\{ - \frac{a_j^2}{2\sigma_{xj}^2} \right\} \tag{36}$$

The conditional probability density function of c_j for given a_j is

$$P(c_j/a_j) = \frac{P(a_j, c_j)}{p(a_j)} = \frac{1}{\sqrt{2\pi}\, \sigma_{yj}\, \sqrt{1-\rho_{xyj}^2}} \exp\left\{ - \frac{1}{2\, \sigma_{yj}^2 (1-\rho_{xyj}^2)} \left(c_j - \rho_{xyj} \frac{\sigma_{yj}}{\sigma_{xj}} a_j \right)^2 \right\} \tag{37}$$

Consequently, the conditional probability density function of c_j for given a_j is also Gaussian with mean $\rho_{xyj} \frac{\sigma_{yj}}{\sigma_{xj}} a_j$ and a standard deviation of $\sigma_{yj} \sqrt{1-\rho^2_{xyj}}$. Similarly, the conditional distribution of d_j for given b_j is Gaussian with mean $\rho_{xyj} \frac{\sigma_{yj}}{\sigma_{xj}} b_j$ and standard deviation of $\sigma_{yj} \sqrt{1-\rho^2_{xyj}}$

The random variable c_j is generated from a Gaussian distribution with mean $\rho_{xyj} \frac{\sigma_{yj}}{\sigma_{xj}} a_j$ and a standard deviation of $\sigma_{yj} \sqrt{1-\rho^2_{xyj}}$

Similarly, the random variable d_j is generated from a Gaussian distribution with mean $\rho_{xyj} \frac{\sigma_{yj}}{\sigma_{xj}} b_j$ and a standard deviation of $\sigma_{yj} \sqrt{1-\rho^2_{xyj}}$

One can now proceed to calculate a point of the random processes, say at time t_1 with

$$x(t_1) = \sum_{j=1}^{n} (a_j \cos \omega_j t_1 + b_j \sin \omega_j t_1)$$

and $$y(t_1) = \sum_{j=1}^{n} \{c_j \cos (\omega_j t_1 + \alpha_j) + d_j \sin (\omega_j t_1 + \alpha_j)\}$$

using expression (33) and $\omega_j = \omega_\ell + (j-1)\,\Delta\omega$

where $\Delta\omega = \frac{\omega_u - \omega_\ell}{n-1}$ for $j = 1, 2, \_ \_ \_ \_ n$.

Next, the following point of the random processes can be calculated at time $t_1 + \Delta t$ and so on. Again the choice of time interval Δt depends on the value of the upper significant wave number and should be such that

$$\Delta t \leq \frac{\pi}{\omega_u}$$

IV. SIMULATION OF THE STREAMWISE STRONG-WIND TURBULENCE COMPONENT

Let the flow field be homogeneous in the horizontal plane and stationary with respect to time. The wind velocity can be resolved into three components, two in the horizontal plane, one of which is along the mean wind direction (x) and one is normal to it (y). The third component is taken vertically upward (z). The instantaneous components can be written in forms of a mean and a fluctuation, so that

$$U(z,t) = \overline{U}(z) + u(z,t)$$

$$V(z,t) = v(z,t)$$

$$W(z,t) = \overline{W}(z) + w(z,t).$$

The estimated spectral density function of the wind speed in the planetary boundary layer for the eastern United States is given by van der Hover (Ref. 11). It shows that the "spectral gap" between 1 cycle per hour to 10 cycles per hour may be used for the stable estimation of $\overline{U}$ and $\overline{W}$ for a sample function with a duration of about 1/2 hour.

Under strong wind conditions, the mixing action of the mechanical turbulence tends to reduce the atmosphere to a state of neutral stability. Consequently, the turbulence near the ground is only due to frictional effects and will vary only significantly with the surface drag and height above the ground. If this is the case, the turbulence can be described as a random process which may be approximated by a stationary Gaussian process with zero mean (Ref. 5).

Two correlated longitudinal turbulence-components at two different locations A and B are simulated. The direction of the separation distance A B is normal to the x coordinate in the horizontal plane and consequently parallel to the y coordinate.

The spectral density function of the longitudinal turbulence-component can be estimated by using Davenport's empirical strong-round spectrum (Ref. 12).

$$S'_u(f) = \frac{4K\,\bar{U}_1^2}{f} \quad \frac{x^2}{[1+x^2]^{4/3}} \tag{38}$$

where f is the frequency in cycles per second. K is the drag coefficient dependent on the surface roughness and $\bar{U}_1$ is the reference mean-velocity near the ground at an elevation of 10 m, so that the shear stress near the ground $\tau' = K \rho \bar{U}_1^2$. The parameter $x = \frac{1200\,f}{\bar{U}_1}$ and $\int_0^\infty S'_u(f)\,df = \bar{u}^2$.

Using the circular frequency ω, where $\omega = 2\pi n$, expression (38) becomes:

$$S'_u(\omega) = \frac{4K\,\bar{U}_1^2}{\omega} \quad \frac{x'^2}{(1+x'^2)^{4/3}}$$

where $x' = \frac{600\,\omega}{\pi\,\bar{U}_1}$ for the range $0 \leq \omega < \infty$

so that $\int_0^\infty S'_u(\omega)\,d\omega = \bar{u}^2$

Hinze (Ref. 13) shows that the auto-correlation coefficient $R'(\tau) = \frac{\overline{u(t)\,u(t+\tau)}}{\bar{u}^2}$ and the energy spectrum function $S'_u(n)$ are Fourier cosine transforms. Using the fact that $R'(\tau)$ and $S'_u(n)$ are even functions and introducing the auto-correlation function $R(\tau) = R'(\tau)\,\bar{u}^2$ and the exponential form one obtains

$$S'_u(\omega) = \frac{1}{\pi} \int_{-\infty}^{\infty} R(\tau)\, e^{-i\omega\tau}\, d\tau \quad \text{and}$$

$$R(\tau) = 1/2 \int_{-\infty}^{\infty} S'_u(\omega)\, e^{i\omega\tau}\, d\omega$$

Now let $S_u(\omega) = 1/2\ S'_u(\omega)$ then

$$S_u(\omega) = \frac{1}{2\pi} \int_{-\infty}^{\infty} R(\tau)\, e^{-i\omega\tau}\, d\tau \qquad \text{and} \tag{40}$$

$$R(\tau) = \int_{-\infty}^{\infty} S_u(\omega)\, e^{i\omega\tau}\, d\omega \tag{41}$$

Expression (40) is used in the previous sections of this report and consequently expression (39) becomes

$$S_u(\omega) = 1/2\ S'_u(\omega) = \frac{2\,K\,\overline{U}_1^{\,2}}{\omega} \frac{x'^2}{(1+x'^2)^{4/3}} \tag{42}$$

Now Davenport's expression for the power spectral density function corresponds to the one as defined before.

Ang and Amin (Ref. 5) suggest an empirical relation for the coherence function for the longitudinal turbulence components at two points separated by a distance Δy parallel to the y coordinate.

$$\gamma(\omega) = \exp\left\{ - \frac{k'\Delta y\, \frac{\omega}{2\pi}}{\overline{U}_1} \right\} \tag{43}$$

where k' is a dimension less coefficient between 20 and 25.

The quadrature spectrum is zero when the cross spectrum is even. For this particular case the maximum correlation between u_A and u_B is expected to occur at a zero lag and consequently the cross-spectral density function is expected to be approximately even. Consequently it is assumed that the quadrature-spectrum function, $Q_{xy}(\omega)$, is zero for all ω.

Figures 2 and 9 show two sets of correlated time series representing the stream wise turbulence components based on Davenport's empirical strong-wind spectrum, the exponential expression for the coherence function (Eq. 43) and a vanishing quadrature spectrum density function. The two time series in Fig. 2 were obtained using the exponential model with

uniformly distributed phase angle. In Fig. 9 the two time series were obtained from the trigonometric model with normally distributed amplitude.

In both cases the number of generated random variables is 600 (n = 600). Davenport's spectrum was evaluated at intervals of $\Delta\omega$ = .005236 rad/sec with a lower wave number cut-off of $\omega_\ell = 0.00377 \frac{\text{rad}}{\text{sec}}$ (0.0006 Hz) and an upper wave number cut-off ω_u = 3.14 rad/sec (0.5 Hz). All simulated turbulence data were evaluated at Δt = 1.0 sec time interval in order to avoid the effect of aliasing. The total length of each of the simulated time series is thirty minutes. The average reference velocity at altitude of 10 m. was taken to be $\overline{U}_1$ = 16.5 m/sec. The drag coefficient K was chosen to be 0.005 and the lateral separation distance Δy was taken at 5 meters.

Figures 4 and 10 show the hystograms of the amplitude of the simulated time series and are approximately Gaussian in nature. However, both sets show a non-zero mean-value which can be attributed to the sample length. With increased sample length the mean value will approach zero. The calculated standard deviation turns out to be of the order of 2.6 m/sec in all four cases. Since Davenport's spectrum seems to be independent of altitude the calculated standard deviations will all be of the order of 2.6 m/sec. which can be attributed to the short-comings of this emperical relation for the spectral density function.

Figures 4 and 11 show the calculated auto-correlation functions for the simulated turbulence data. For a time-lag τ = 0 of course, the variance of the time series which is the square of the standard deviation must be obtained. For all four time series this requirement was extremely well satisfied. As a rule of thumb, it is considered to be desirable to keep the maximum time lag less than one-tenth of the sample size (Ref. 7).

In figures 5 and 12 the calculated cross-correlation function is shown. Since it was assumed that the quadrature spectrum for the two sets of turbulance data vanished for all ω, the cross-correlation function must be symmetrical such that $R_{xy}(\tau) = R_{yx}(\tau)$. By comparison of the sets of cross-correlation function this requirement seems to be adequately satisfied.

Figures 6 and 13 show the calculated spectral density function and Davenport's emperical spectrum from which the time series were obtained. For the first method the agreement is very good but for the second method the agreement seems not so good. However, the degree of agreement depends on the particular sample realization of the time series. One must keep in mind that the calculated spectrum function is strictly an estimator of the strictest definition of the spectral density function.

Figures 7 and 14 show the calculated cospectra and quadrature spectra. The calculated quadrature spectra should theoretically be zero for all frequencies. However, because of the relatively small sample length (30 min.) of the time series one may expect non-zero values for the quadrature spectra at low frequencies.

The coherence functions for the two sets of simulated turbulence data are shown in figures 8 and 15. By nature of the definition of the coherence function, one may expect large deviation from the emperical expression for the coherence function. It must be remembered that the results given in this report are based on a single set of sample realizations of relatively short duration. Consequently, the calculated functions are simply estimators of the required statistical quantities. The accuracy of these estimators can be improved by using more sample realizations or evaluating the random processes for a longer sample time.

Based on the above results for the two different methods, no significant differences can be found. However, the simulation technique utilizing the trigonometric model with normally distributed amplitudes is more adaptable to the simulation of many correlated random processes simultaneously.

REFERENCES

1. Goto, H., Doki, K. and Akiyoshi, T., "Artificial Earthquake Waves by Computer," Proceedings of Japan Earthquake Engineering Symposium, 1966.

2. Housner, G. W., and Jennings, P. C., "Generation of Artificial Earthquakes," Journal of the Engineering Mechanics Division, ASCE, Vol. 90, Feb., 1964.

3. Amin, M. and Ang, A.H.S., "Nonstationary Stochastic Model of Earthquake Motions," Journal of the Engineering Mechanics Division, ASCE, Vol. 94.

4. Liu, S.C., "Dynamics of Correlated Random Pulse Trains," Journal of the Engineering Mechanics Division, ASCE, Vol. 96, August, 1970.

5. Ang, A.H.S. and Amin, M., "Probabilistic Structural Mechanics and Engineering," Notes of NSF Summer Institute University of Illinois, June, 1970.

6. Parzen, E., "Modern Probability Theory and Its Applications," John Wiley.

7. Bendat, J. S. and Piersol, A. G., "Measurement and Analysis of Random Data," John Wiley.

8. Hoshiya, M. and Spence, S. T., "Reliability Analysis of a Tainter Gate," Proceedings of JSCE, No. 183, Nov. 1970.

9. Hoshiya, M., "Response of a Single Degree of Freedom System with Probabilistic Parameters," Proceedings of JSCE, No. 188, April, 1971.

10. Shinozuka, M. and Sato, Y., "On the Simulating Method of Earthquakes and the Response of Structure," Proceedings of Japan Earthquake Engineering Symposium, 1966, pp. 167-172.

11. Van der Hoven, "Power Spectrum of Horizontal Wind Speed in the frequency Rame from 0.0007 to 900 cycles per hour," Journal of Meteorology, Vo. 14, 1957, p. 160.

12. Davenport, A. G., "The Spectrum of Horizontal Gustiness near the Ground in High Winds," Journal of Royal Meteorological Society, Vol. 87, No. 372, April 1961, pp. 191-211.

13. Hinze, J. O., "Turbulence," McGraw Hill.

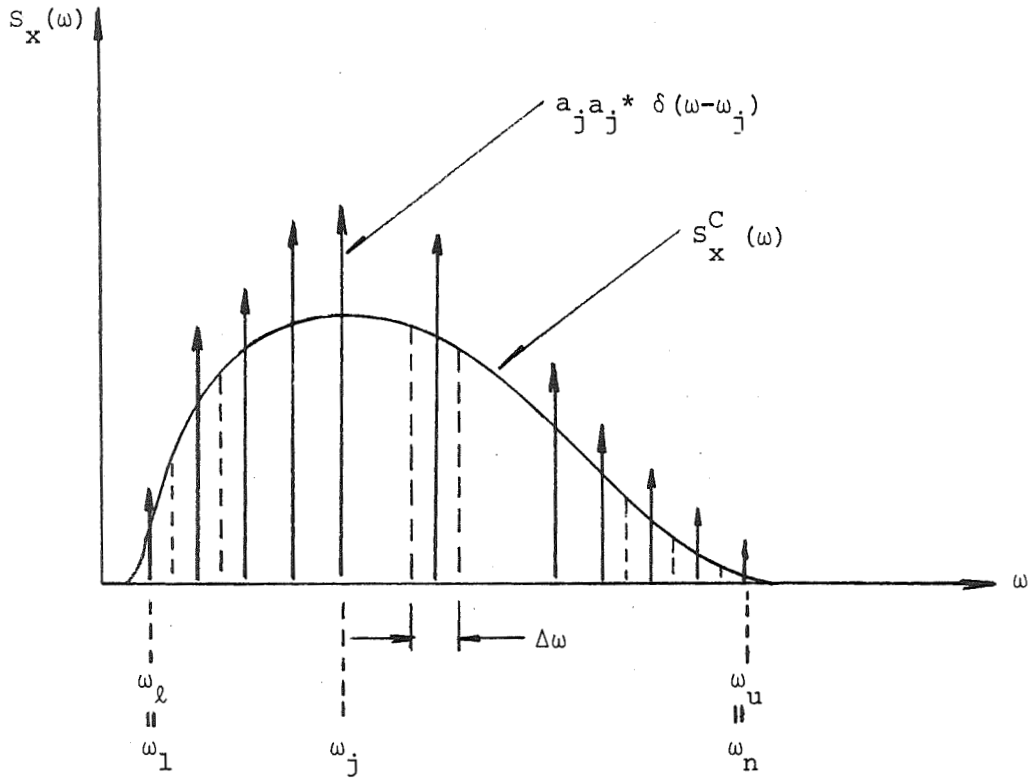

Fig. 1. Schematic sketch of the continuous and discrete spectrum

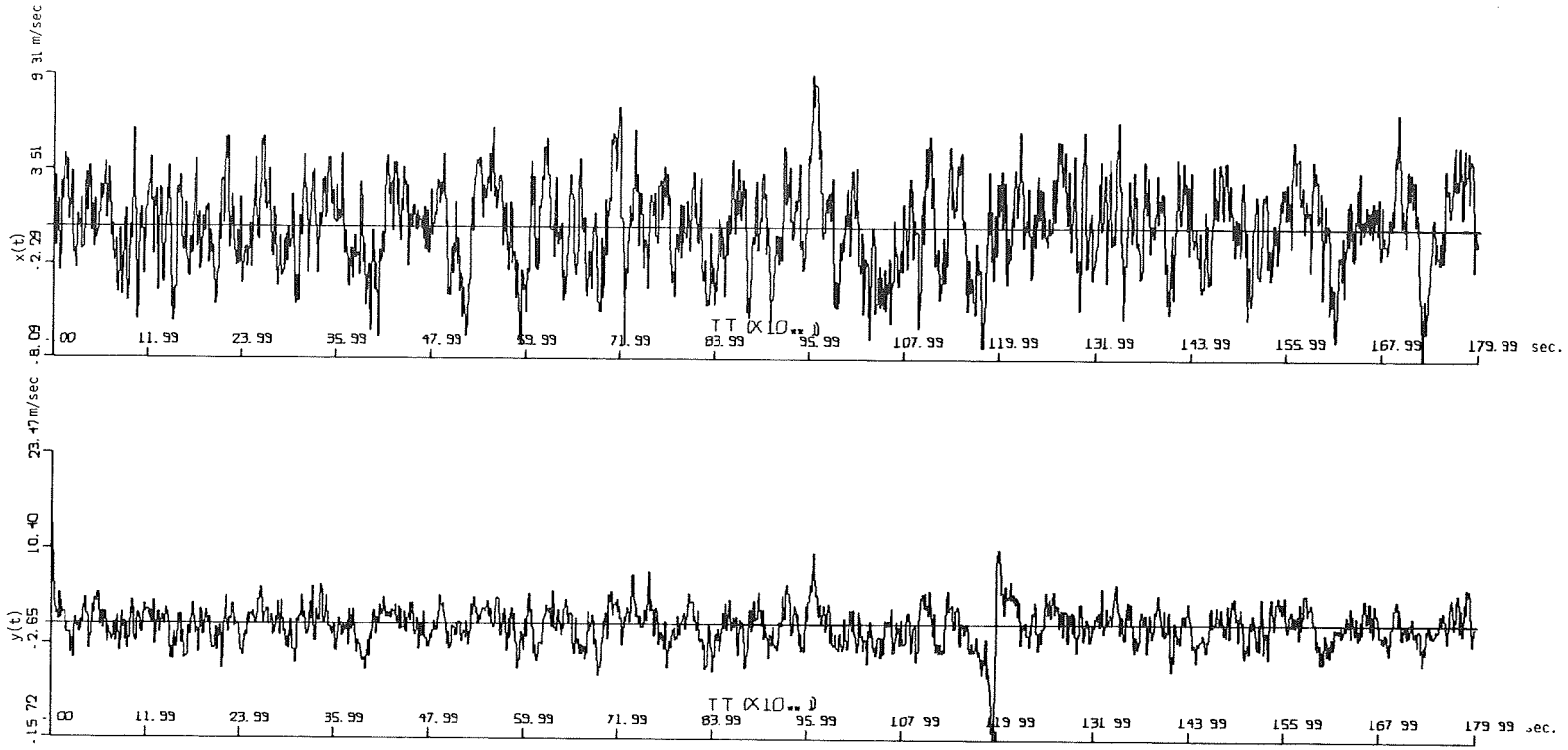

Fig. 2. Set of correlated time series representing the stream wise turbulence component using simulation method No. 1 (Random phase angle)

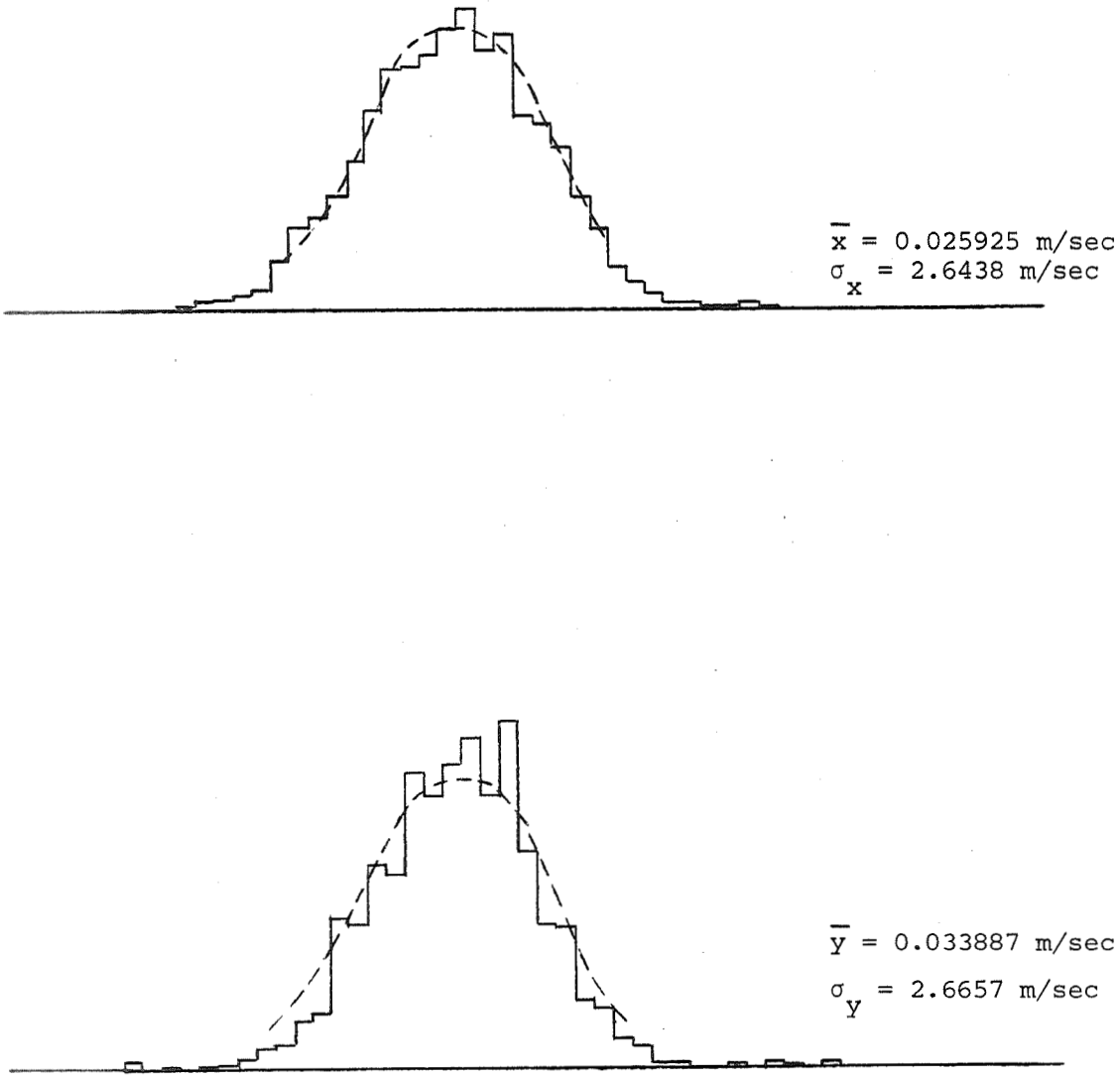

Fig. 3. Hystograms of amplitude of time series of Fig. 2. Dashed curve represents the normal probability density function

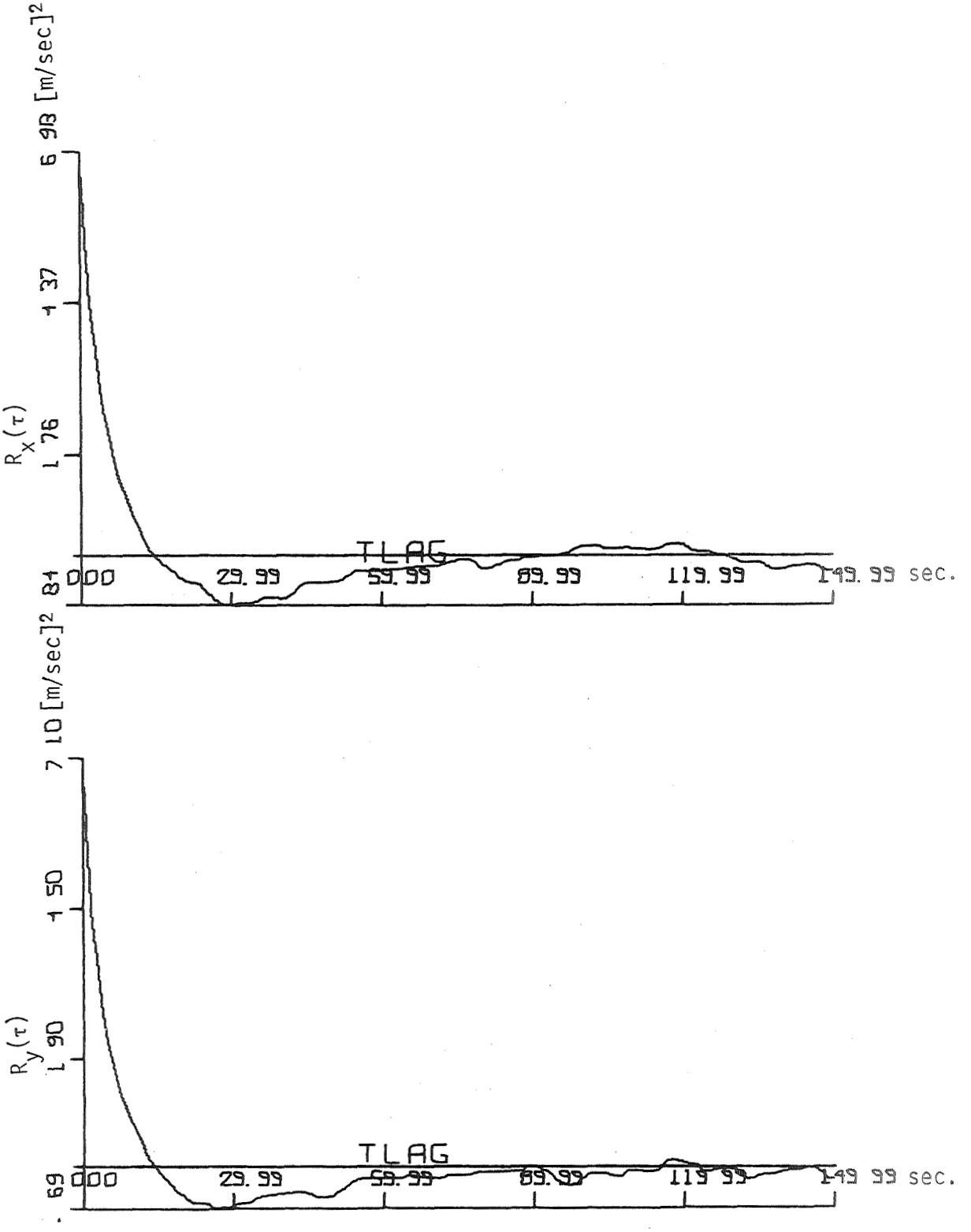

Fig. 4. Calculated autocorrelation functions of time series of Fig. 2

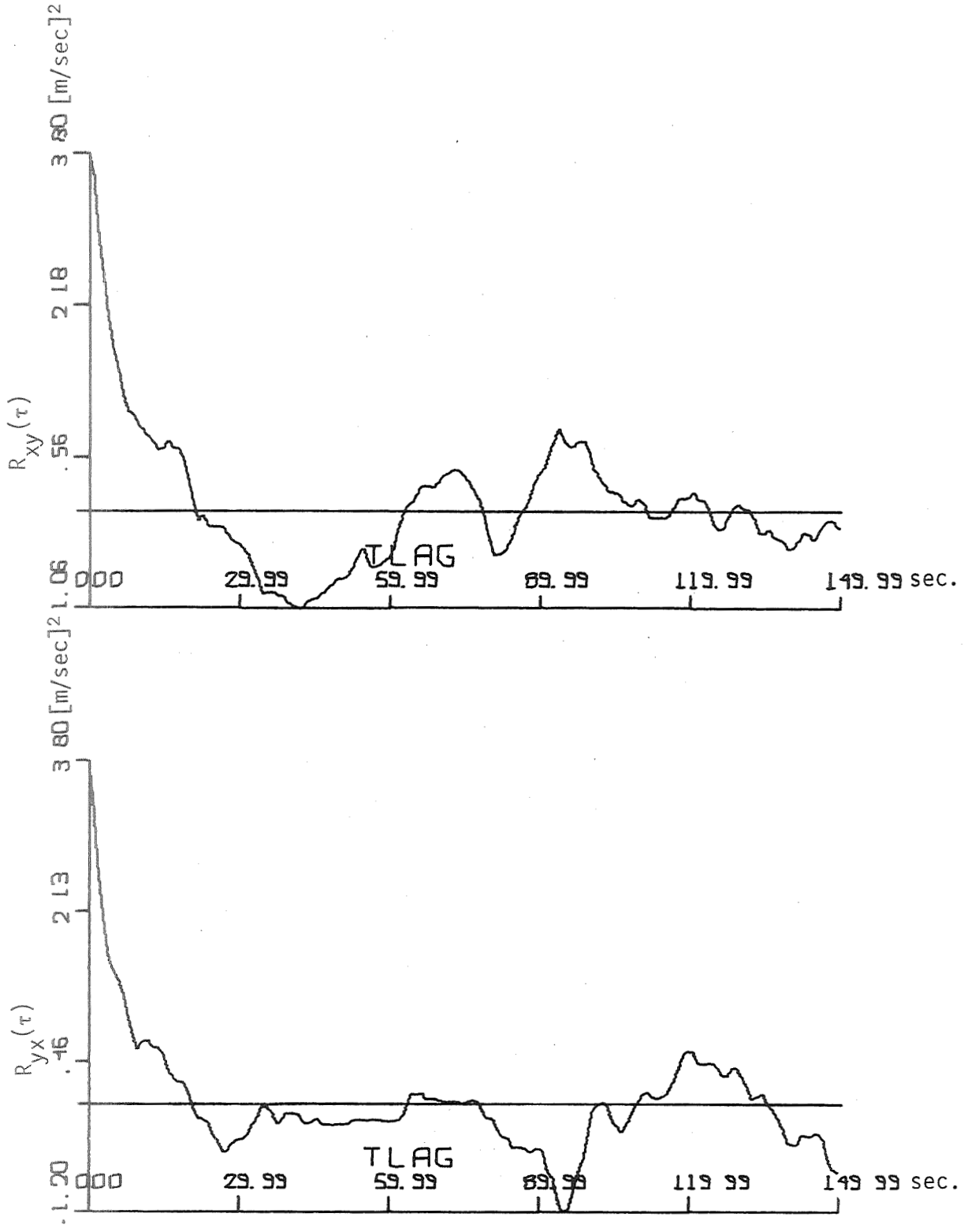

C
Fig. 5. Calculated cross-correlation functions of time series of Fig. 2

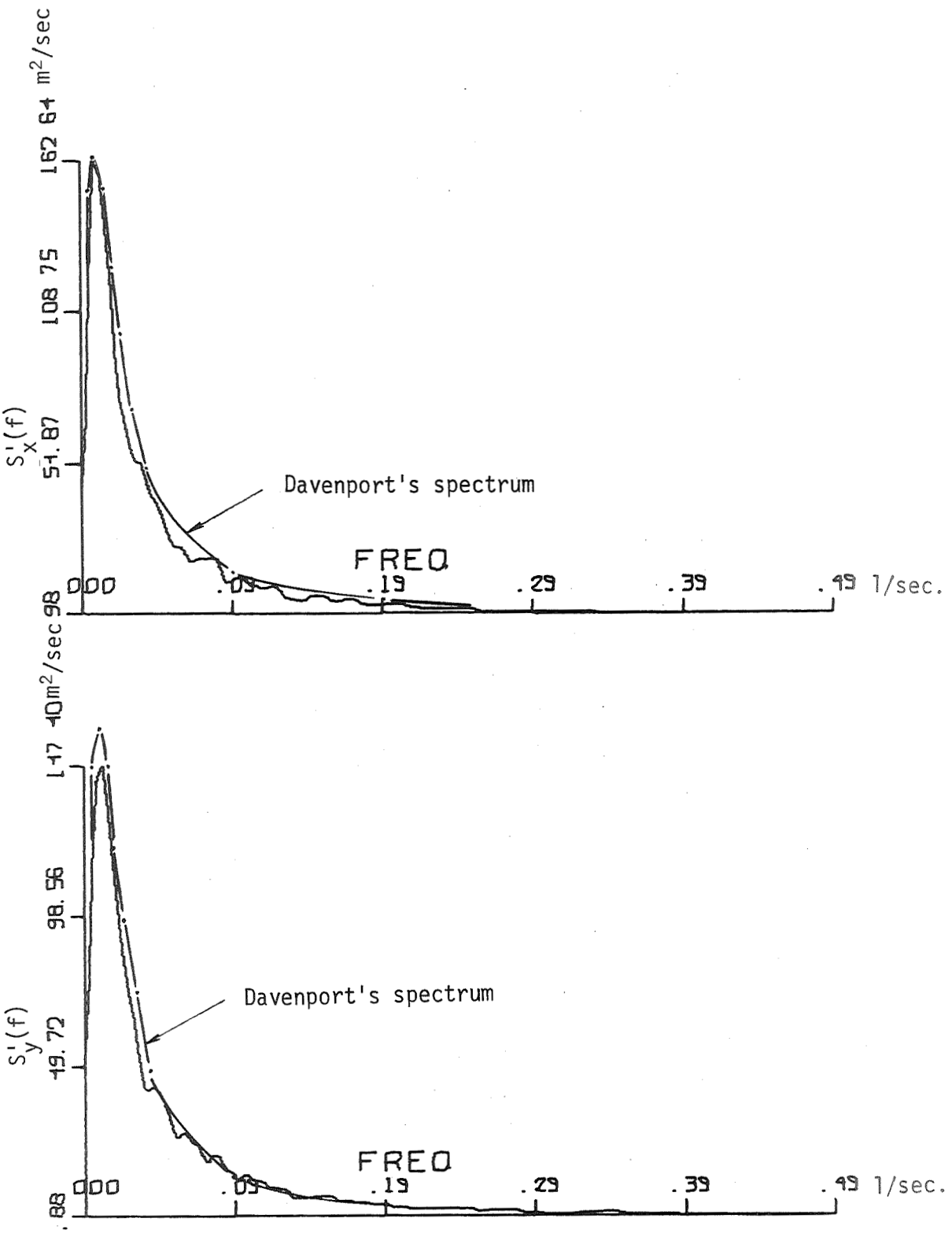

Fig. 6. Calculated spectra of time series of Fig. 2

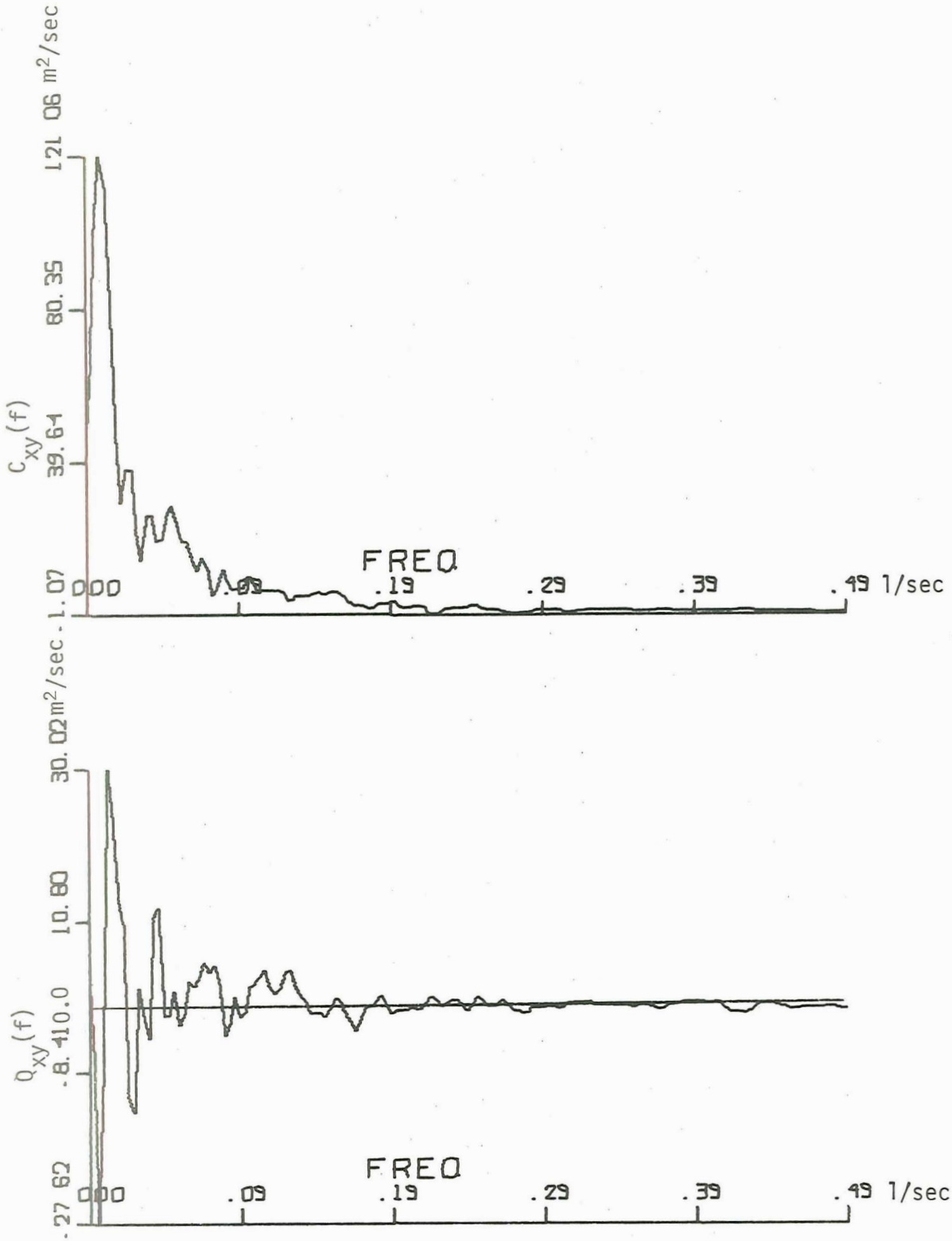

Fig. 7. Calculated co-spectrum and quadrature spectrum of time series of Fig. 2

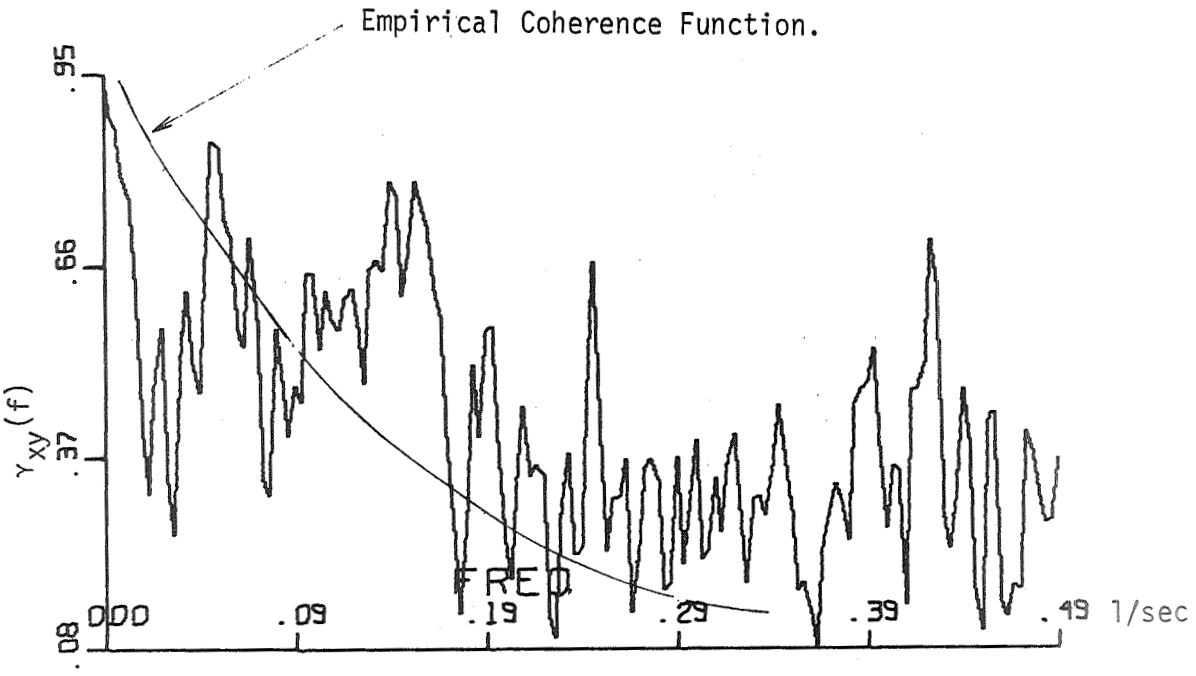

Fig. 8. Calculated coherence function of time series of Fig. 2

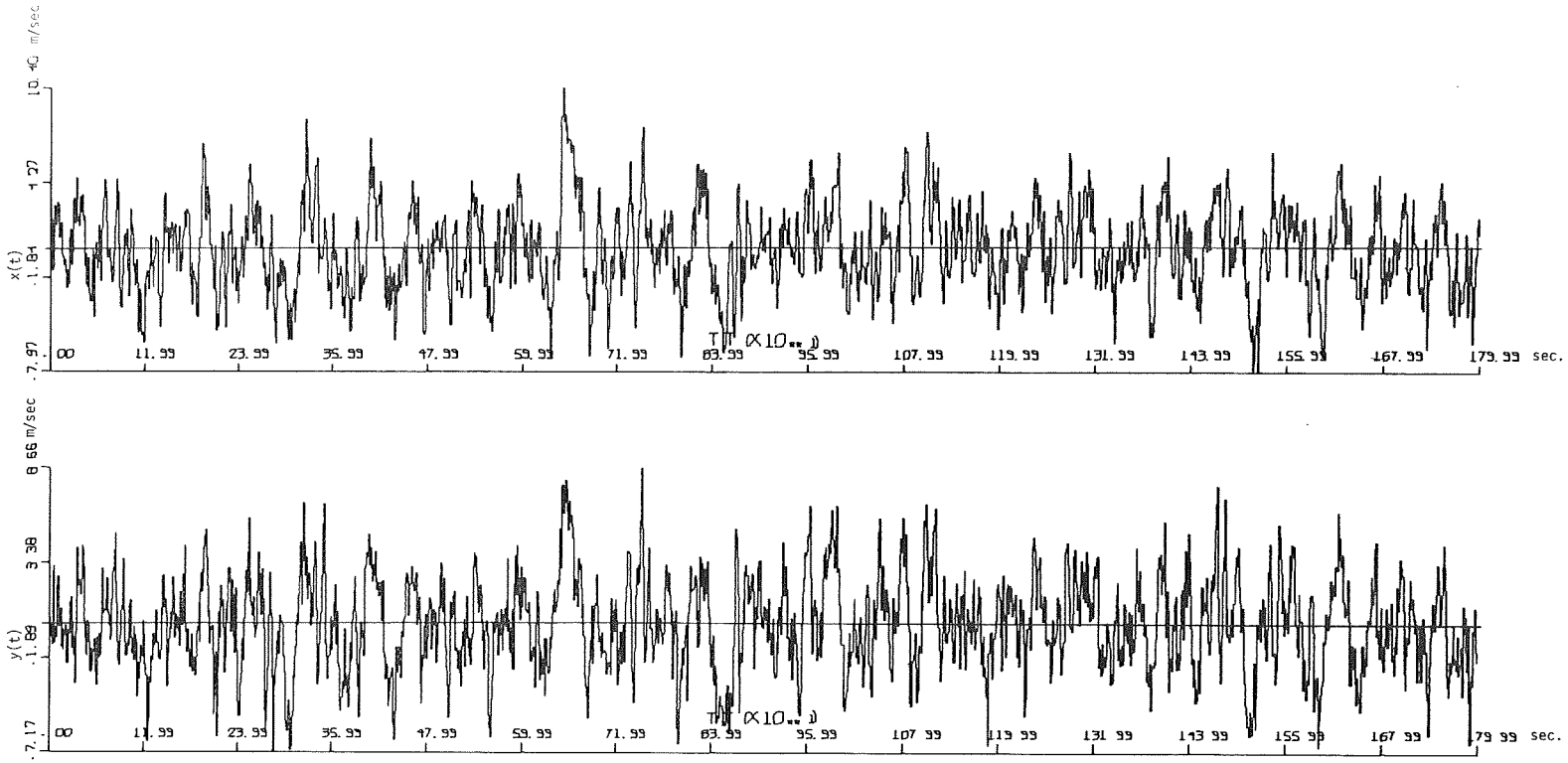

Fig. 9. Set of correlated time series representing the stream wise turbulence component using simulation method No. 2 (Random amplitudes)

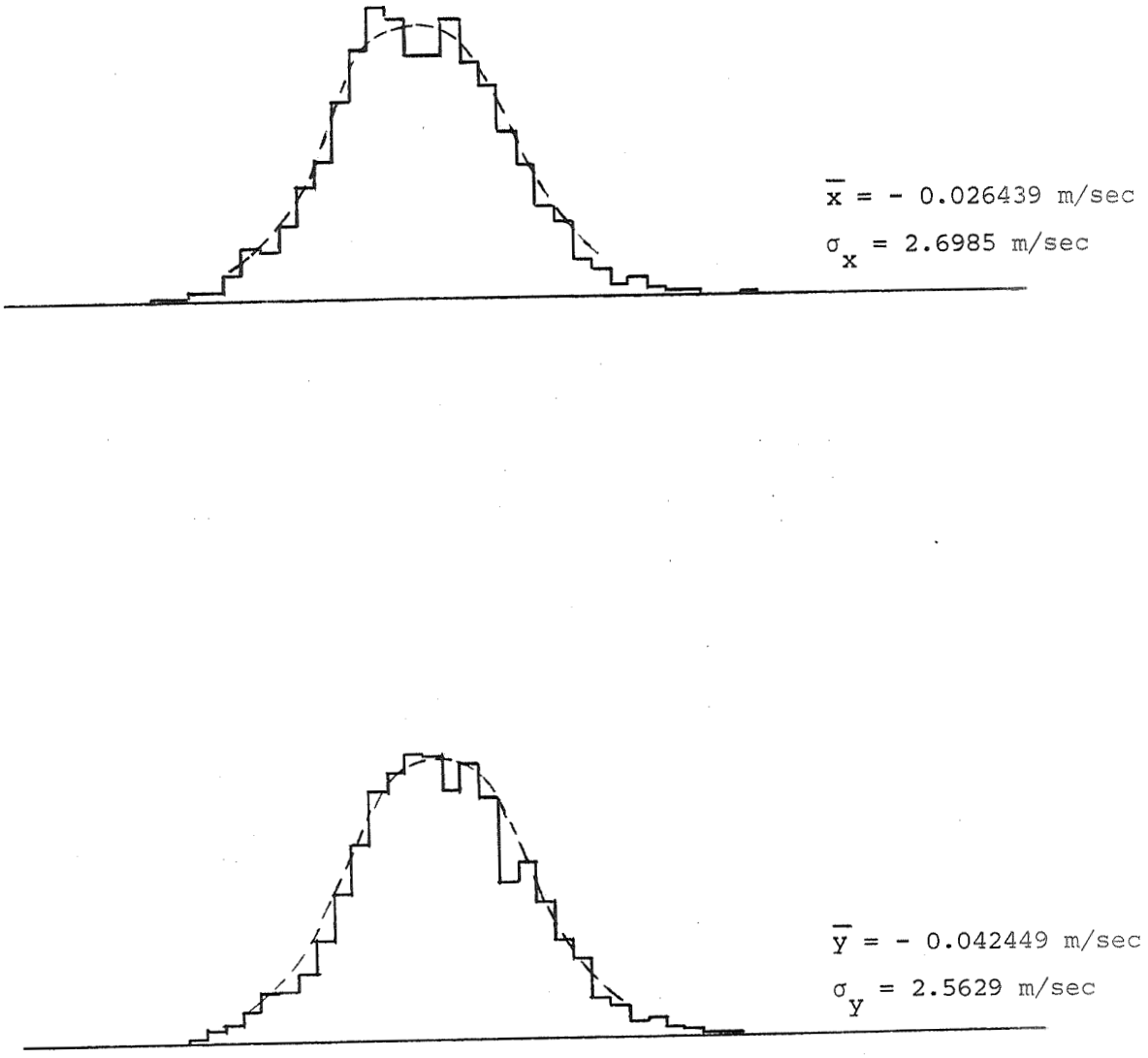

Fig. 10. Hystograms of amplitude of time series of Fig. 9
Dashed curve represents the normal probability density function

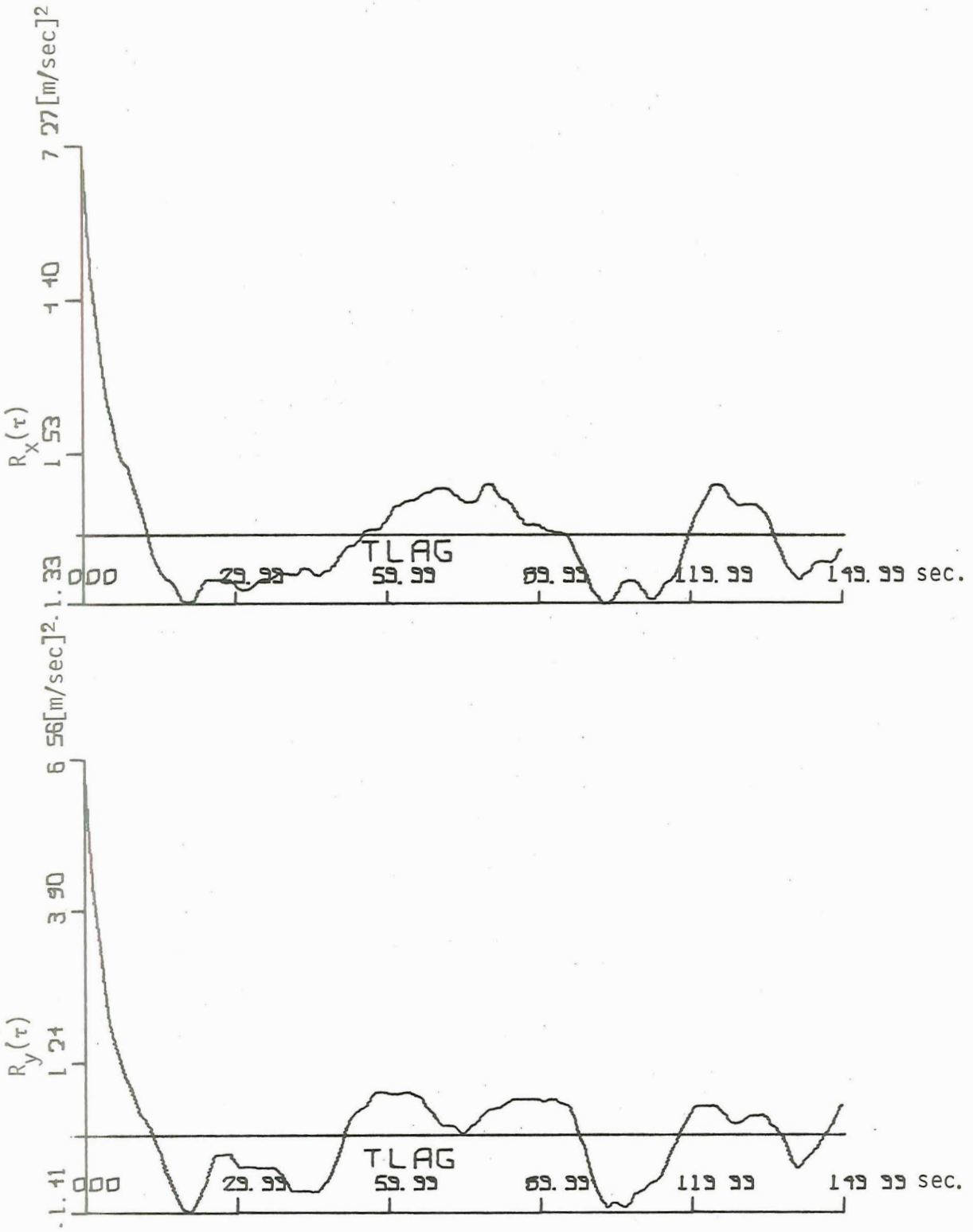

Fig. 11. Calculated autocorrelation function of time series of Fig. 9

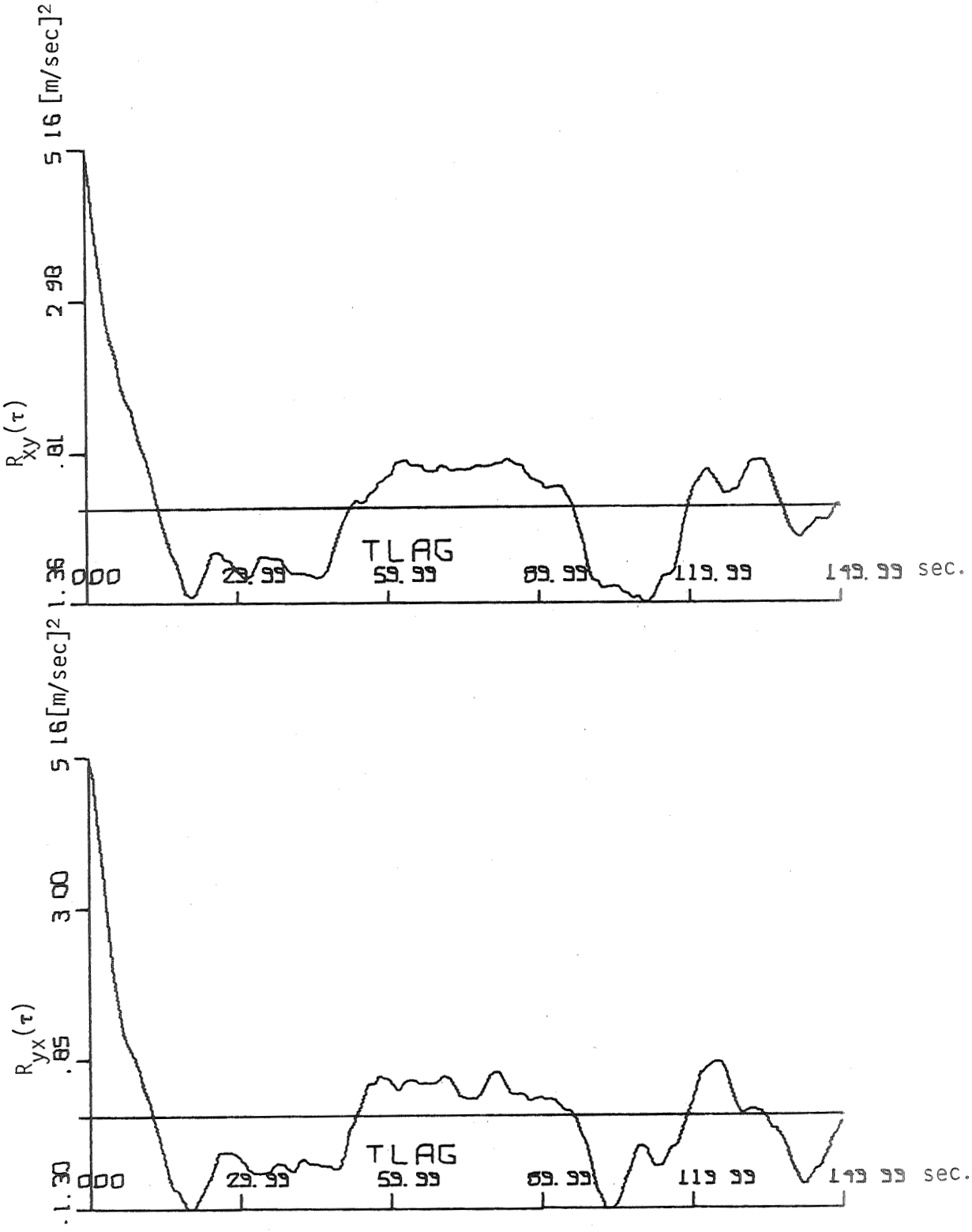

Fig. 12. Calculated cross-correlation functions of time series of Fig. 9

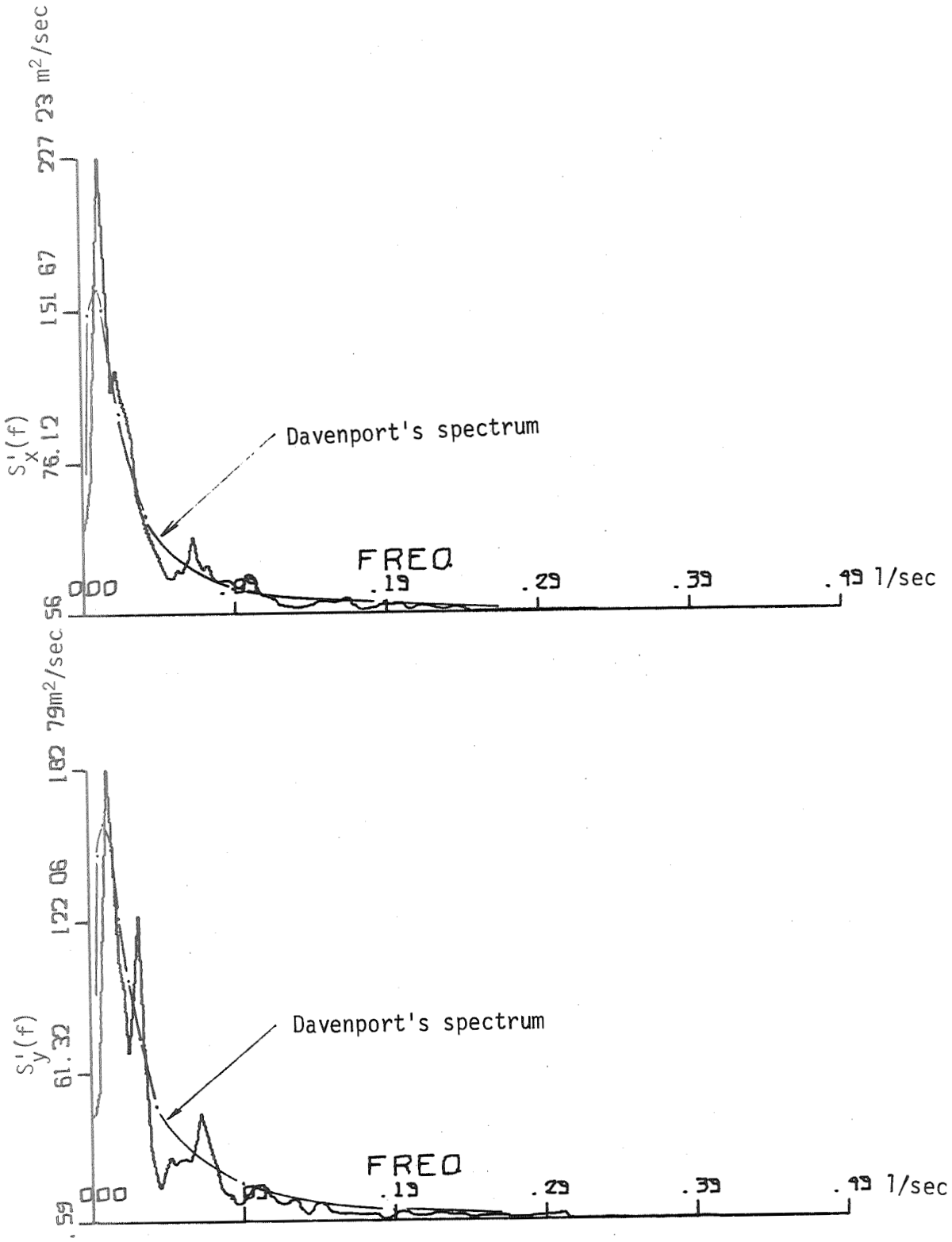

Fig. 13. Calculated spectra of time series of Fig. 9

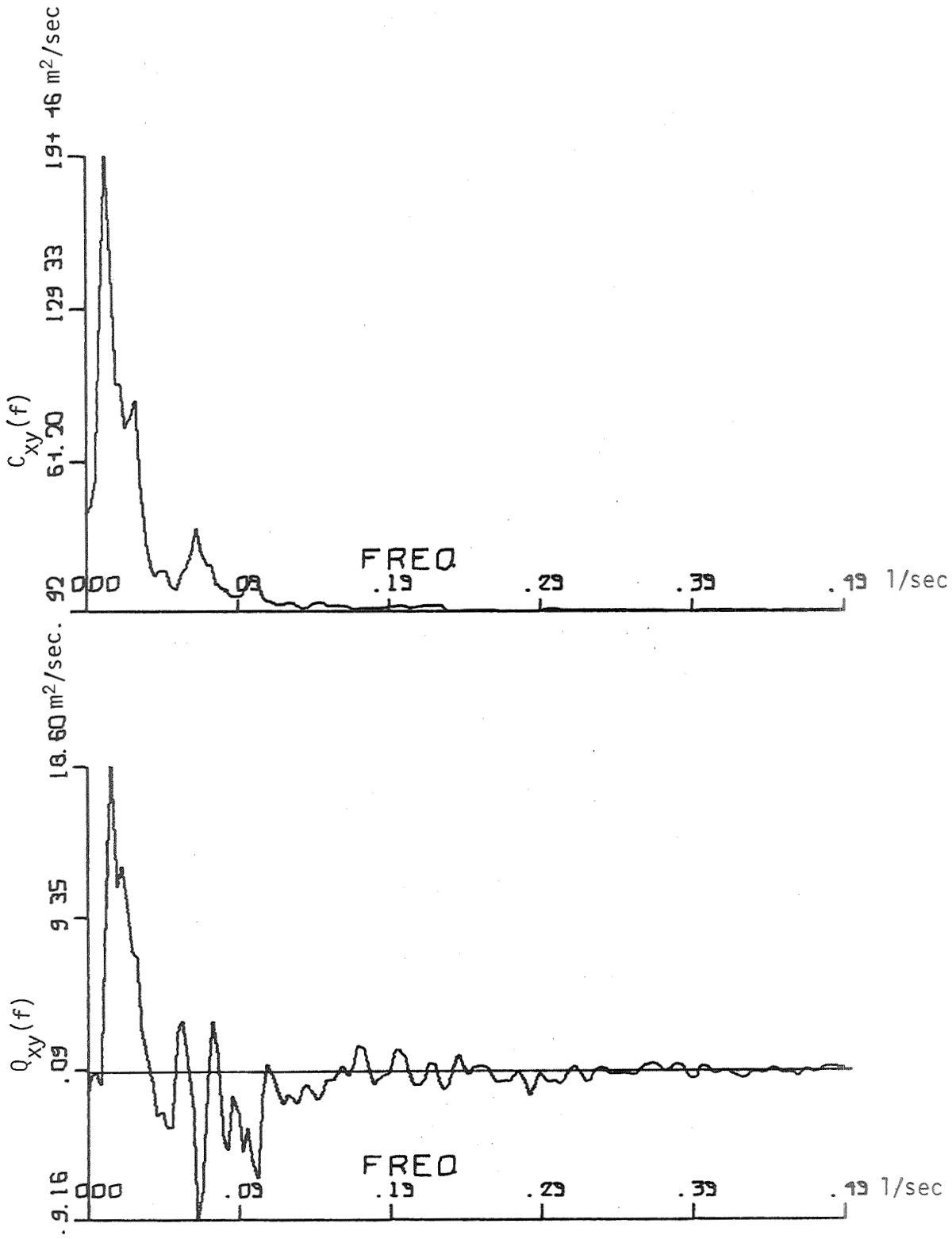

Fig. 14. Calculated co-spectrum and quadrature spectrum of time series of Fig. 9

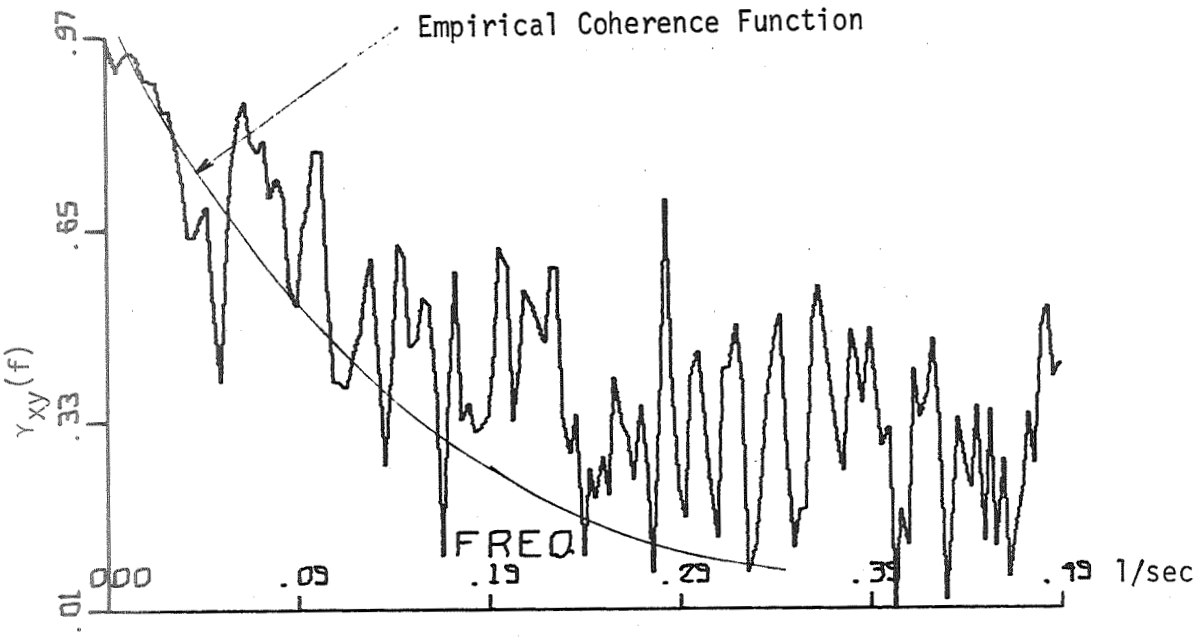

Fig. 15. Calculated coherence function of time series of Fig. 9

SPECIAL DISTRIBUTION

Office of Scientific and Technical Information (5 copies)
National Aeronautics and Space Administration
Washington, D. C. 20546

Mr. C. H. Carter (1 copy)
University Affairs Office
National Aeronautics and Space Administration
Washington, D. C. 20546

Mr. W. A. McGowan (1 copy)
OART
National Aeronautics and Space Administration
Washington, D. C. 20546

Wallops Station
National Aeronautics and Space Administration
Wallops Island, Virginia 23337

Mr. R. L. Krieger, Director (1 copy)
Mr. A. D. Spinak, Associate Director (1 copy)
Mr. M. W. McGoogan (1 copy)
Mr. W. H. West (1 copy)
Mr. J. W. Gray (1 copy)
Mr. J. F. Spurling (1 copy)

Dr. G. H. Fichtl (1 copy)
George C. Marshall Space Flight Center
Aerospace Environment Division
Huntsville, Alabama 35812

Mr. H. C. S. Thom (1 copy)
Senior Research Fellow
Gramax Building, Room 704
8060 13th Street
Silver Spring, Maryland 20910

Engineering Research Center
Colorado State University
Fort Collins, Colorado 80521

Dr. J. E. Cermak (1 copy)
Professor V. A. Sandborn (1 copy)

Dr. R. D. Marshall (1 copy)
National Bureau of Standards
Building Research Division
Washington, D. C. 20234

Dr. Toshie Okumura (1 copy)
Professor of Civil Engineering
University of Tokyo
Bunkyo-Ku, Tokyo JAPAN

Dr. Manabu Ito (1 copy)
Associate Professor of Civil Engineering
University of Tokyo
Bunkyo-Ku, Tokyo JAPAN

Dr. Haresh C. Shah (1 copy)
Asscciate Professor of Civil Engineering
Stanford University
Stanford, California 94305

Dr. Alfred H. S. Ang (1 copy)
Professor of Civil Engineering
University of Illinois
Urbana, Illinois 46990

Dr. John LePore (1 copy)
Assistant Professor of Civil Engineering
University of Pennsylvania
Philadelphia, Pennsylvania 19104